UDK 67.017:669.715:54-143:54-48
Original scientific article/Izvirni znanstveni članek

ISSN 1580-2949
MTAEC9, 52(5)583(2018)

EFFECT OF MELT TREATMENT ON THE MICROSTRUCTURE AND MECHANICAL PROPERTIES OF AN AA3003 ALUMINUM ALLOY

VPLIV NAČINA OBDELAVE TALINE NA MIKROSTRUKTURO IN MEHANSKE LASTNOSTI ALUMINIJEVE ZLITINE AA3003

Guiqing Chen[1], Gaosheng Fu[2], Tianyun Wei[1], Chaozeng Cheng[2], Shaoyi Lin[1], Lili Song[2]

[1]Fujian Chuanzheng Communications College, Department of Mechanical Engineering, no. 112 Shoushan Road, Fuzhou 350007, China
[2]Fuzhou University, College of Materials Science and Engineering, no. 2 Xueyuan Road, Fuzhou 350108, China
fugaosheng@fzu.edu.cn

Prejem rokopisa – received: 2017-12-05; sprejem za objavo – accepted for publication: 2018-03-22

doi:10.17222/mit.2017.207

The AA3003 aluminum-alloy melt was treated with different types of melt treatment, and the effect of the melt treatment on the microstructure and mechanical properties of the alloy was investigated. The results show that the impurity content of the untreated (UT) AA3003 aluminum alloy reached 0.6801 %. Its structure contains two kinds of particles, β-Al (FeMn) and α-Al (MnFeSi), whose distributions look like long strips, massive and skeletal forms, reducing the strength and plastic toughness of the material. After the efficient integrated treatment (EIT), the impurity content of the alloy decreased significantly, and the fluidity of the aluminum melt was improved, which is conducive to the role of a refiner, refining the cast grain size. An addition of La and Ce during the EIT eliminates the presence of the harmful second-phase Mn (MnFe) Si and Al (FeMn) distributed at the grain boundaries. The grain boundaries become stable, and the heat resistance and high-temperature performance of the alloy are improved, which is advantageous for the hot-deformation processing. The purity of the AA3003 aluminum alloy is significantly improved with the EIT, which is conducive to the subsequent grain refinement and modification so that the metallurgical quality of the alloy is significantly improved. Its mechanical properties at room temperature and after a thermal deformation are superior to those of the AA3003 aluminum alloy processed with the conventional integrated treatment (CIT).

Keywords: AA3003 aluminum alloy, melt treatment, purity, metallurgical quality, mechanical properties

Avtorji prispevka so talino Al zlitine AA3003 obdelovali na različne načine in raziskovali njihov vpliv na mikrostrukturo in mehanske lastnosti te zlitine. Rezultati raziskave so pokazali, da je bila vsebnost nečistoč v neobdelani (UT; angl.: untreated) AA3003 zlitini 0,6801 %. V strukturi zlitine sta se nahajali dve vrsti delcev, β-Al (FeMn) in α-Al (MnFeSi), ki so bili po zlitini porazdeljeni v obliki dolgih trakov. Te masivne skeletne oblike delcev zmanjšujejo trdnost in žilavost materiala. Po učinkoviti integrirani obdelavi taline (EIT; angl.: efficient integrated treatment) se je vsebnost nečistoč občutno zmanjšala, izboljšala se je tekočnost taline in posledično je prišlo do udrobljenja zlitine (zmanjšanja velikosti zrn). Dodatek La in Ce med EIT je odstranil škodljivo Mn fazo (MnFe), tako da sta se Si in Al (FeMn) porazdelila po kristalnih mejah. Kristalne meje tako postanejo stabilne in izboljšajo se mehanske lastnosti zlitine pri povišanih temperaturah, kar je prednost pri nadaljnjih postopkih vroče deformacije. Čistost Al zlitine AA3003 se je močno povečala z EIT, kar je vodilo do učinkovitega zmanjšanja velikosti kristalnih zrn in občutnega izboljšanja metalurške kvalitete zlitine. Njene mehanske lastnosti so bile pri sobni temperaturi po termični deformaciji precej boljše, kot jih dosežemo pri Al zlitini AA3003 s konvencionalno integrirano toplotno obdelavo (CIT, angl.: conventional integrated treatment).

Ključne besede: Al zlitina vrste AA3003, obdelava taline, čistost, metalurška kvaliteta, mehanske lastnosti

1 INTRODUCTION

As oxide inclusions, gases, impurities and other metallurgical defects inevitably exist in aluminum ingots and other raw materials during a smelting process, an aluminum melt is easily oxidized, reacting with air so that the metallurgical quality of the aluminum melt is not high,[1,2] being congenitally deficient. It directly affects the final quality of a product and its processing performance; at the same time, it also has a negative impact on the solidification and other processes, and the role of the solid-state treatment is annihilated. Therefore, to improve the quality of aluminum, metallurgy is extremely important.[3] If these defects are not promptly removed during the casting process, the following processes (such as rolling, extrusion, heat treatment, surface treatment, etc.) improve the material, but it is later difficult to eliminate the effects of the inclusions and gas. They directly affect the formability of a material, and it is difficult to ensure the quality of various high-performance aluminum products.

With the development of lightweight and thin-wall products, the impact of the metallurgical quality (defects) will be even more prominent. Therefore, it is very important to improve the technical level of aluminum-alloy casting (especially the purification, deterioration and grain refinement and other melt treatments). It has played a key role in improving the metallurgical quality and deformation performance of various aluminum materials and has become an important way to explore the potential performance of traditional materials and develop new materials. The theory and technology of melt treatment have also become key scientific and technical

problems in the preparation and use of high-performance aluminum.[4,5] For AA3003 aluminum sheets, aluminum ingots in excellent raw conditions have a decisive effect on the subsequent processing and final product performance, and the original state of the alloy is closely related to the melt-treatment process.[6–8] In order to study in detail the influence of the original-state microstructure characteristics of the alloy on the subsequent thermal deformation, AA3003 aluminum ingots were prepared using three types of melt treatment. The influences of the melt treatment on the metallurgical quality and performance were analyzed to provide the basis for establishing the intrinsic relationship between the original state of the alloy and its thermal deformation behavior.

2 EXPERIMENTAL PART

The main components of the AA3003 aluminum alloy are (*w*/%): 0.62 Fe, 0.58 Si, 1.09 Mn, 0.068 Cu, 0.006 Ti, 0.03 Mg, 0.007 Ni, 0.008 Zn, the balance being Al. The preparation of the ingots: aluminum ingots were subjected to the following melt treatments in a graphite-crucible resistance furnace:[9] the conventional integrated treatment (CIT) and efficient integrated treatment (EIT); one ingot was left untreated (UT). The CIT uses a commercial refining flux, the Al5TiB refiner and RE metamorphism. The EIT uses an in-house-produced high-efficiency purification flux, the Al5TiB refiner and RE metamorphism. Ingots of 110 mm × 20 mm × 70 mm were cast into a metal mold and then annealed at 510 °C for 20 h. The amount of inclusions in the samples was determined with the flux-rinse method. After a sample was polished, it was etched with a 0.5–2 % HF solution for 5–10 min. An XJL-05 horizontal metallographic microscope and a QHS-2200 three-dimensional video microscope were used to observe the inclusion morphology. The homogenized microstructure was observed using XL30-ESEM scanning electron microscopy (SEM), and the composition of the second phase was identified with an EDAX32 energy dispersive spectrometer (EDS). A plate-shaped specimen of (1.6 × 15 × 30) mm was processed using a DK7725B EDM CNC wire-cutting machine. Tensile testing was performed on an INSTRON-1185 material-testing machine.

Cylindrical specimens of 10 mm in diameter and 15 mm in height were machined for hot-compression tests. Both flat ends of the specimens were recessed to a depth of 0.2 mm to entrap the graphite powder in order to minimize the friction between the specimen surface and the clamp. The samples were mounted onto a Gleeble-1500 thermal simulator for an isothermal constant-strain-rate hot-compression test. The experimental conditions for the hot deformation were as follows: the heating rate of the samples was controlled at 1 °C/s; the insulation took 5 min after the set temperature; the control of the amount of compression deformation was 0.7. The deformed specimens were quenched in water quickly after each compression test in order to maintain the microstructure. The microstructures of the deformed samples were observed using JEM-2100F transmission electron microscopy (TEM). For microscopic examinations, the specimens were mechanically polished and etched with Keller's reagent (2.5 mL HNO_3, 1.5 mL HCl, 1 mL HF and 95 mL H_2O). The foils used for TEM were prepared by mechanically polishing them to less than 80 μm and then punched into 5-mm discs. Finally, a twin-jet electro-polishing device was used to prepare the samples with an electrolyte solution of 25 % nitric acid and 75 % methanol at a voltage of ~15 V DC and a temperature below –20 °C. It is worth noting that the TEM samples were sprayed continually until a small hole appeared. An HVS-1000 Vickers-microhardness tester was used to measure the microhardness of the simulated-hot-compression specimens. After the deformation, they were cooled down to room temperature and the microhardness was tested. The load was 0.49 N. The load-holding time was 30 s. The average microhardness of a sample was obtained after five points were tested.

3 RESULTS AND DISCUSSION

3.1 Effect of the melt treatment on inclusions and grain microstructure

Figure 1 shows the microstructure of the AA3003 aluminum alloy after three types of the melt treatment

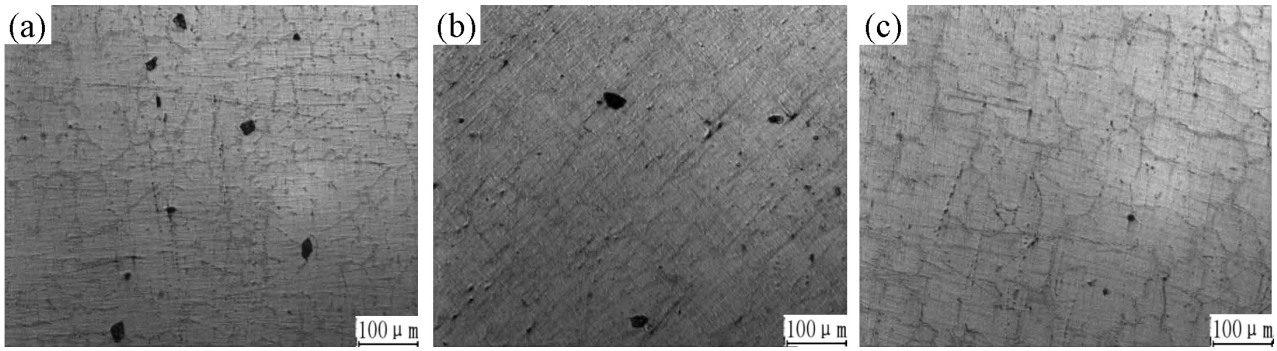

Figure 1: Cast microstructure (polished) of the AA3003 aluminum alloy: a) UT, b) CIT, c) EIT

were used in the polished state. The inclusions revealed with the flux-rinse method are shown in **Table 1**.

Table 1: Inclusions in the AA3003 aluminum alloy (as-cast)

Melt-treatment process	UT	CIT	EIT
Inclusions (%)	0.6801	0.3616	0.0967
Inclusion-removal rate (%)	–	46.83	85.78

The inclusion content in the AA3003 aluminum alloy left UT was 0.6801 %, and the sizes of different inclusions were uneven. The CIT process reduced the inclusion content to 0.3616 %, the removal rate was 46.83 %, and the coarse inclusions can still be seen. This is related to two factors: on the one hand, the RE modifiers used in this experiment are rarely added, although RE leads to impurity removal and decontamination. On the other hand, the main component of the added RE is La, and studies have shown that La cannot reduce the influence of other impurity elements, except the Fe and Si elements, and cannot change its existence mode.[10] After the EIT process, the inclusion content in the alloy was significantly reduced (0.0967 %), the inclusion-removal rate was 85.78 %, and the size and distribution of the inclusions were small and uniform. This is because the EIT uses a highly efficient inclusion-removing flux (CJ-5) for the filtration purification, whose purification principle is to organically combine aluminum melting, highly efficient inclusion removing and filtering. The design and optimization of the composition of the flux are based on the thermodynamics and kinetics conditions for removing inclusions. It fully exerts the purifying effect, removing the inclusions, and creates favorable kinetics conditions for the subsequent degassing purification, which is in accordance with the purifying principle of relying mainly on the removal of inclusions while degassing is a subsidiary process.[11]

Table 2: Average grain size of AA3003 aluminum alloy

Melt-treatment process	UT	CIT	EIT
Average grain size (μm)	94	63	51

The microstructures of the AA3003 aluminum alloy obtained with LM are shown in **Figure 2**. **Table 2** shows the average grain size measured with the image-analysis system.

The average grain size of the UT AA3003 aluminum alloy was the largest; after the CIT, the grain size decreased. Although the Al_5TiB grain refiner was added during the CIT process, the average grain size was still coarse due to a high content of inclusions, which was unfavorable for the role of a refiner. On the other hand, after the EIT, the grain size of the AA3003 aluminum alloy was the smallest and the distribution of the structure was more uniform. The grain refinement was carried out on the basis of efficient purification of the EIT. The melt-purification treatment changed the size and morphology of TiB_2 in the original structure of the refiner.[12] It helped to spread the core of the nucleation and remove the insoluble core. After the EIT, the insoluble inclusions and aggregates were obviously reduced so that the viscosity of the aluminum melt was reduced and the fluidity improved. The effective nucleation core (such as $TiAl_3$, TiB_2, etc.) in a refiner can be diffused uniformly in the aluminum melt, which is conducive to the role of refiners. As a result, after the EIT, the grain size of an ingot is significantly lower than that obtained with the CIT.

3.2 SEM observation and a composition analysis

The microstructure and the composition analysis of the UT AA3003 aluminum alloy are shown in **Figure 3**. **Table 3** shows a summary of the analysis results for the second-phase chemical composition from **Figure 3**.

Table 3: Second-phase chemical composition of the UT AA3003 aluminum alloy (*w*/%)

Phase shape	Al	Mn	Fe	Si	Name of the compound	Fe/Mn	
Long stripes	A	98.8	0.3	0.5	–	Al(FeMn)	1.67
	B	96.8	0.8	1.9	–	Al(FeMn)	2.28
Skeletal shape	C	98.7	0.4	0.5	–	Al(FeMn)	1.25
Block	D	96.6	0.9	1.9	–	Al(FeMn)	2.11
Plum blossom	E	97.1	0.3	1.6	0.6	Al(MnFe)Si	5.33

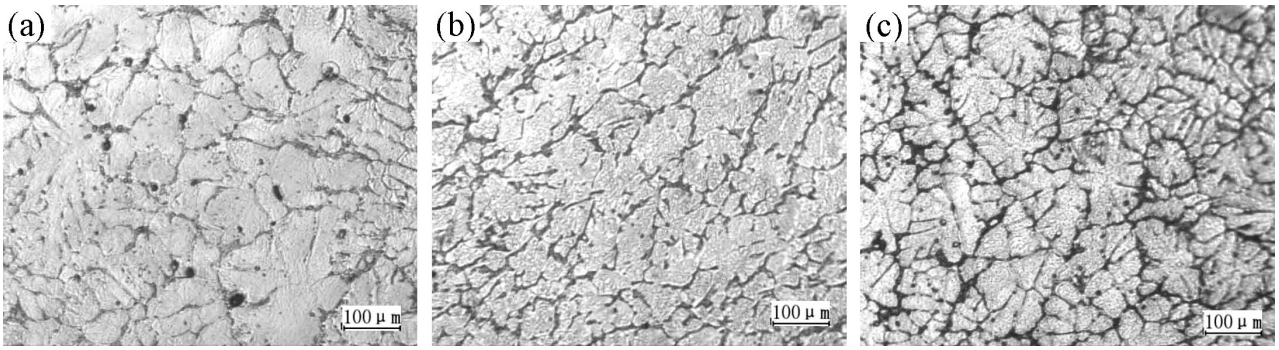

Figure 2: LM images of AA3003 aluminum alloy after different melt treatments: a) UT, b) CIT, c) EIT

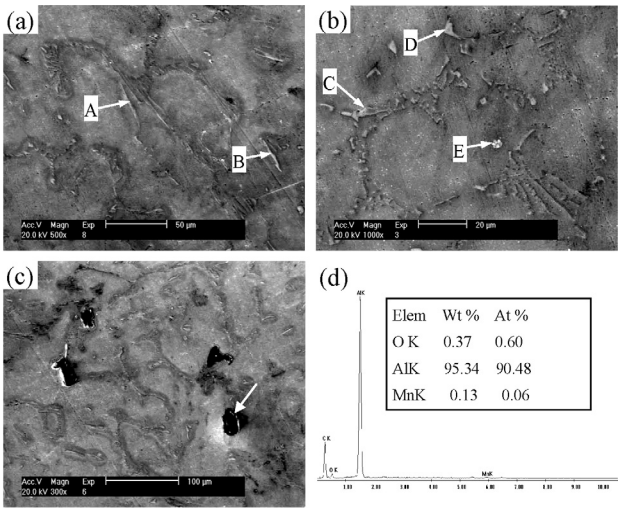

Figure 3: SEM images show the morphology of the UT AA3003 aluminum alloy: a) 500×, b) 1000×, c) 300×, d) composition of the inclusion (EDS) marked with the arrow in c)

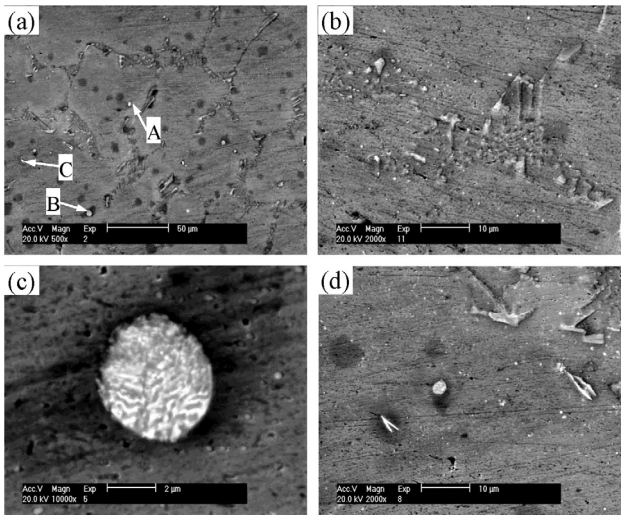

Figure 4: SEM images show the morphology of the AA3003 aluminum alloy after EIT: a) 500×, b) 2000×, c) enlarged view of B (10000×), d) enlarged view of C (2000×)

As can be seen from **Figure 3** and **Table 3**, there are two main components of the second phase, the first type is the Al (FeMn) phase, which is large, skeletal and containing long strips; the second type is the Al (MnFe) Si phase, whose distribution was plum-like. The above two phases contain Mn because the main alloying element in the AA3003 aluminum alloy is Mn. Most of the Mn is dissolved in α-Al in the supersaturated form, and part of the Mn forms a compound, which is distributed in the form of second-phase particles near the grain boundaries or among the dendritic arms. This is related to two factors: on the one hand, during the casting process, the cooling rate is very fast, the diffusion coefficient of Mn atoms is small, and the diffusion activation energy is large, so the Mn dissolved in α-Al is supersaturated. On the other hand, since the solid solubility of Mn in Al is large, decoupling cannot be carried out during the homogenization treatment. The solid solubility of Fe is smaller than that of Si, which more likely forms a second phase. Therefore, the two main types of second-phase particles normally presented in the AA3003 aluminum alloy are β-Al (FeMn) and α-Al (MnFeSi), and the relative content of the two particle types depends on the specific alloy composition and the solidification rate.[13]

The alloy has a large amount of second phases, including long strips, massive and skeletal forms in the vicinity of the grain boundaries of the alloy or dendritic arms. They are separated from the matrix and have a different coefficient of expansion, elastic modulus and hardness from the metal matrix. The second phase is prone to stress concentration at sharp corners, and it strongly hinders the normal flow of α-Al in the deformation process.[14,15] It is also easily broken by itself and easily forms microcracks and uneven deformation zones with α-Al; thereby, the strength and toughness are significantly reduced.

Figure 4 shows the microstructure and the oxidized inclusions of the AA3003 aluminum alloy after the EIT. **Table 4** shows the corresponding second-phase chemical composition obtained with EDS.

The second phases after the EIT are much smaller than that of the untreated sample, having a scattered distribution. There are two main types: the first type is the Al (MnFe) SiRE phase, which has a spherical distribution, as shown in **Figure 4c**. The second type is the AlSiRE phase, which has a small-V shape distribution, as shown in **Figure 4d**. The two types of the second phase contain Si, indicating that the addition of RE can effectively reduce the solid solution of Si atoms. At the same time, the shape of the second phase in the alloy is also changed, which is related to the metamorphism of the added RE during the EIT. It can change the Fe-phase morphology.

The new phase – Al (MnFe) SiRE – appears in the AA3003 aluminum alloy after the addition of RE modifiers, which are spherical and refined. The reason for the formation of Al (MnFe) SiRE is the fact that the tendency of an intermediate compound to form in the alloy is related to the chemical activity of the alloying

Table 4: Second-phase chemical composition of the AA3003 aluminum alloy after EIT (*w*/%)

Phase shape		Al	Mn	Fe	Si	La	Ce	Compound	Fe/Mn
Spherical	A	97.0	0.3	1.0	0.6	0.5	0.3	Al(MnFe)SiRE	3.33
	B	96.7	0.1	0.2	0.9	1.0	0.4	Al(MnFe)SiRE	2.0
Small-V shape	C	96.6	–	–	0.7	1.4	0.7	AlSiRE	–

element, that is, the greater the electronegativity difference of the alloying element, the greater is the possibility of forming an intermediate compound.[16] The electronegativity of RE elements La and Ce is about 1.1, the electronegativity of Fe and Si is about 1.8, while the main alloying element (Mn) of the AA3003 aluminum alloy has an electronegativity of 1.5. In this way, the electronegativity difference between La, Ce and the impurity elements (Fe and Si) is larger than the value for Mn so that an affinity for Fe and Si is more likely to occur, and it is easier for an intermetallic compound to be formed. It can also be seen from **Table 4** that the average amount (0.59 % and 0.73 %) of Fe and Si in spherical Al (MnFe) SiRE is higher than that of Mn (0.16 %). The phases of Al (FeMn) and Al (MnFe) Si were changed to form the new phase (Al(MnFe)SiRE) after the RE was added. According to the Hume-Rothery rule relating to the alloy phase, the formation of a stable mesophase (compound) in the alloy limits the solid solubility of the primary solid solution. Therefore, the formation of the Al(MnFe)SiRE phase reduces the amount of Fe and Si in the AA3003 aluminum alloy, and of course also the solid solubility of Mn.

Based on the above analysis, the addition of La and Ce changes the original solid solution of Si and Fe to a certain extent and eliminates the existence of the harmful second phases (Al(MnFe)Si and Al(FeMn)) distributed at the grain boundaries. It stabilizes the grain boundaries, improves the heat resistance and high-temperature performance of the alloy, which is advantageous for the hot-deformation processing.

3.3 Effect of the melt treatment on mechanical properties

Table 5 shows the mechanical properties of the AA3003 aluminum alloy treated with different melt treatments at room temperature. It can be seen that the mechanical properties were improved after different melt treatments. Especially in the case of the AA3003 aluminum alloy treated with EIT, the most obvious improvement was noticed, when the strength increased by 41.66 % and the elongation increased by 45.63 %.

Table 5: Mechanical properties of the AA3003 aluminum alloy at room temperature

Melt-treatment process	Tensile strength (MPa)	Increase rate (%)	Tensile elongation (%)	Increase rate (%)
UT	123.44	–	22.42	–
CIT	139.22	12.78	26.13	16.55
EIT	174.86	41.66	32.65	45.63

As can be seen from **Table 1**, the impurity-removal rate of the EIT increased by 38.95 % compared with the CIT, thereby the alloy after the EIT process shows more excellent mechanical properties. This is because the oxidized inclusions in the solidified structure of the aluminum alloy severely rupture the continuity of the material matrix, and the oxidized inclusions are often attachments of hydrogen, so the alloy is liable to generate pores and looseness.[17,18] Under the action of the tensile stress, inclusions, shrinkage and pores have a greater stress concentration, and are easy to become sources of cracks. With an increase in the content of inclusions, the number of micro-defects in the alloy increases, and a low average pitch of defects makes the crack-propagation resistance smaller. Micropores are easy to germinate, grow and aggregate, making the casting easy to crack and fracture. In the process of tensile deformation, inclusion particles seriously hinder the normal flow of the plastic deformation of a material due to a large hardness difference between the hard and brittle oxidized inclusions and the aluminum alloy matrix.[19–21] At the same time, microcracks and uneven deformation zones can be easily formed between the hard and brittle oxidized inclusions and the alloy matrix, and a brittle fracture easily occurs under stress. The existence of these micro-defects accelerate the material-breaking process, eventually leading to decreased mechanical properties of materials.

The grain size (D) of the alloy and the yield strength (σ_y) are in line with the Hall-Petch relationship in Equation (1):

$$\Delta\sigma_y = k\Delta\frac{1}{\sqrt{D}} \propto \Delta\frac{1}{\sqrt{D}} \quad (1)$$

where k is the material constant.

According to the data from **Table 2**, the average grain size of the AA3003 aluminum alloy after different melt treatments is reduced. Based on Equation (1), it can be concluded that the smaller the average grain size, the higher is the yield strength of the alloy. The average grain size of the AA3003 aluminum alloy after the EIT is not significantly different from that of the CIT. Therefore, inclusions mainly have a major effect on the mechanical properties.

According to the previous study of the research group, hot-deformation best temperature of the 3003 aluminum alloy is around 400 °C.[8] Therefore, the microhardness values for the 3003 aluminum alloy with different melt treatments at 400 °C were compared. The relationship between the microhardness of the alloy after hot deformation and the melt treatment process can be obtained, as shown in **Table 6**.

Table 6: Microhardness of the AA3003 aluminum alloy at 400 °C

Melt-treatment process	Strain rate (s^{-1})			
	0.01	0.1	1.0	10.0
UT	42.6	44.8	47.1	49.6
CIT	40.5	43.5	46.2	47.7
EIT	43.8	46.2	49.2	50.6

From **Table 6**, it can be seen that under the same hot-deformation conditions, the AA3003 aluminum alloy with the EIT has the highest microhardness; the second

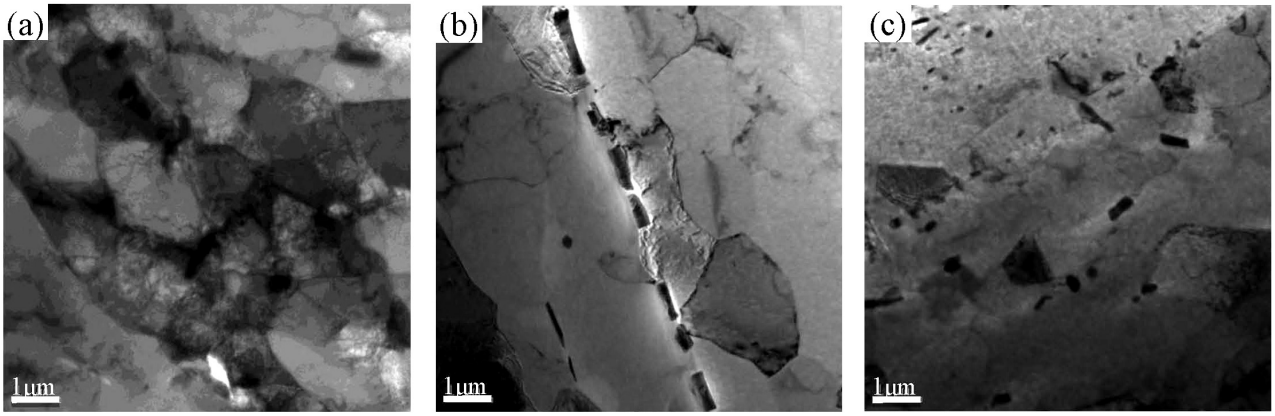

Figure 5: TEM images of the second phase at 400 °C, 0.1 s^{-1}: a) UT, b) CIT, c) EIT

is the UT sample, and the lowest is the CIT sample. This is not only related to the grain size of the hot deformation but also to the strengthening mechanism of the second phase in the alloy. There are two main types of the strengthening mechanism for the second phase:[22,23]

1) When slip dislocations pass through deformable particles with the shear-through mechanism, the increase in the intensity (σ_{PC}), the volume fraction (f) and the particle size (d) of the second phase satisfy the following relationship:

$$\sigma_{\mathrm{PC}} \propto f^{1/2} d^{1/2} \tag{2}$$

2) When slip dislocations pass the non-deformable particles with the Orowan mechanism, the relationship among the increase in the intensity (σ_{PO}), the volume fraction (f) and the particle size (d) of the second phase is as follows:

$$\sigma_{\mathrm{PO}} \propto f^{1/2} d^{-1} \tag{3}$$

According to the analysis from Section 3.2, there is a large number of second-phase particles containing Mn in the AA3003 aluminum alloy. After hot deformation, they are dispersedly distributed along the subgrain boundaries, at which large amounts of dislocations accumulate. Due to the existence of the second-phase particles, the migration of dislocations during the hot deformation is hindered. Once the particles are not deformable, the dislocation line begins to bend. When the dislocation line bending intensifies, the dislocation lines around the particles offset each other due to the opposite sign, producing a dislocation loop surrounding the particles. When each dislocation line passes through the second-phase particles in the above manner, in addition to some resistance, due to the dislocation loops and the reaction of the stress field, impeding effects on the subsequent dislocations are further increased, resulting in the proliferation of dislocations, which has an enhanced effect on the alloys. The second phase of the AA3003 aluminum alloy with the EIT is the smallest; its distribution resembles small rods, spheres and small-V shapes (**Figure 5c**). According to Equation (3), the microhardness of the AA3003 aluminum alloy with the EIT is the highest. The content of the inclusions of the UT AA3003 aluminum alloy is the highest, the volume fraction of the second phase after the hot deformation is large and some hard spots are formed, which make the microhardness of the UT AA3003 aluminum alloy higher than that of the CIT sample.

4 CONCLUSIONS

1. After the EIT process, the inclusion content is reduced and the flowability of the aluminum melt is improved. The effective nucleation core in the refiner is dispersedly distributed, which is beneficial to the effectiveness of the refiner.

2. β-Al(FeMn) and α-Al (MnFeSi) in the forms of skeletal, long strips or large blocks exist in the UT AA3003 aluminum alloy, reducing the strength and toughness of the material. After the EIT, the shape of the second phase changes, the grain boundaries are stabilized, the heat resistance and high-temperature performance of the alloy are improved, which is beneficial to the hot-deformation process.

3. Compared with the CIT, the removal rate increased with the EIT by 38.95 %, and the tensile strength and tensile elongation at room temperature increased by 28.88 % and 29.08 %, respectively, indicating that the purity of the aluminum melt has a key effect on the mechanical properties of the alloy.

4. The internal metallurgical quality of the AA3003 aluminum alloy is significantly improved with the EIT so that the grain size after hot deformation is the smallest and the second phase is finely dispersed. This treatment has an alloy-strengthening effect. As a result, the AA3003 aluminum alloy treated with the EIT has the highest microhardness after hot deformation and good mechanical properties.

Acknowledgments

The authors would like to acknowledge the financial support from the Fujian Natural Science Foundation

(2017J01156, 2017J01083), Xinjiang Uygur Autonomous Region university scientific research program, scientific research key project (XJEDU2016I068), Transportation Science and Technology Project of Fujian Province (200944), and the Materials Nearly Net Forming and Digital Manufacturing Technology Service Team of the Fujian Chuanzheng Communications College of China.

5 REFERENCES

[1] Y. L. Chen, G. S. Fu, W. Z. Chen, Influence of melt-treatment on material constants of aluminum sheet used for easy-open can during hot deformation, Trans. Nonferrous Met. Soc. China, 16 (**2006**) 3, 304–310, doi:10.1016/S1003-6326(06)60052-6

[2] G. Chen, G. Fu, H. Chen, W. Yan, C. Cheng, Z. Zou, Comparative study of the influence of various melt-treatment methods on hot deformation behavior of 3003 Al alloy, Met. Mater. Int., 18 (**2012**) 1, 129–134, doi:10.1007/s12540-012-0015-0

[3] Q. Wang, H. Geng, F. Wang, X. Lin, C. Wang, Effect of parameters of thermal-rate treatment of melt on iron-containing phases in alloy Al – 15% Si – 2.7% Fe, Met. Sci. Heat Treat., 58 (**2016**) 7–8, 405–410, doi:10.1007/s11041-016-0025-5

[4] W. Khalifa, Y. Tsunekawa, M. Okumiya, Effect of reheating to the semisolid state on the microstructure of the A356 aluminum alloy produced by ultrasonic melt-treatment, Solid State Phenomena, 141–143 (**2008**), 499–504, doi:10.4028/www.scientific.net/SSP.141-143.499

[5] G. I. Eskin, Improvement of the structure and properties of ingots and worked aluminum alloy semifinished products by melt ultrasonic treatment in a cavitation regime, Metallurgist, 54 (**2010**) 7–8, 505–513, doi:10.1007/s11015-010-9331-0

[6] G. Chen, G. Fu, W. Yan, C. Cheng, Z. Zou, Mathematical model of dynamic recrystallization of aluminum alloy 3003, Met. Sci. Heat Treat., 55 (**2013**) 3–4, 220–225, doi:10.1007/s11041-013-9609-5

[7] G. Chen, G. Fu, S. Lin, C. Cheng, W. Yan, H. Chen, Simulation of flow of 3003 aluminum alloy under hot compressive deformation, Met. Sci. Heat Treat., 54 (**2013**) 11–12, 623–627, doi:10.1007/s11041-013-9560-5

[8] G. Chen, G. Fu, H. Chen, C. Cheng, W. Yan, S. Lin, Optimization of a hot deformation process of the 3003 aluminum alloy by processing maps, Met. Mater. Int., 18 (**2012**) 5, 813–819, doi:10.1007/s12540-012-5010-y

[9] G. S. Fu, W. Z. Chen, K. W. Qian, Synthetical technique of high-efficient melt-treatment of aluminum and its effect, Chinese J. Nonfer. Met., 12 (**2002**) 2, 269–274, doi:10.3321/j.issn:1004-0609.2002.02.014

[10] G. Yang, J. C. Chen, Y. Du, Y. H. Li, Effects of La on microstructures of industrial pure aluminum, Nonferrous Metals (Extractive Metallurgy), 2 (**2006**) 38–40, doi:10.3969/j.issn.1007-7545.2006.02.012

[11] G. S. Fu, J. X. Kang, W. Z. Chen, Theoretical bases and ways of improving the effect of purification of molten aluminium, Light Alloy Fabrication Technology, 30 (**2002**) 6, 43–51, doi:10.3969/j.issn.1007-7235.2002.06.004

[12] F. Pan, X. Chen, T. Yang, T. Liu, J. Mao, W. Luo, Q. Wang, J. Peng, A. Tang, B. Jiang, A novel approach to melt purification of magnesium alloys, J. Magnes. Alloys, 4 (**2016**) 1, 8–14, doi:10.1016/j.jma.2016.02.003

[13] A. Taþkesen, K. Kütükde, Optimization of the drilling parameters for the cutting forces in B4C-reinforced Al-7xxx-series alloys based on the Taguchi method, Materials and technology, 47 (**2013**) 2, 169–176

[14] A. Biswas, D. J. Siegel, D. N. Seidman, Compositional evolution of Q-phase precipitates in an aluminum alloy, Acta Mater., 75 (**2014**), 322–336, doi:10.1016/j.actamat.2014.05.001

[15] G. Q. Chen, G. S. Fu, H. L. Chen, W. D. Yan, C. Z. Cheng, Z. C. Zou, Research on hot deformation behavior of 3003 Al alloy prepared by different melt-treatment methods, Applied Mechanics and Materials, 66–68 (**2011**), 1611–1616, doi:10.3969/j.issn.1007-2012.2011.04.006

[16] K. Hantzsche, J. Bohlen, J. Wendt, K. U. Kainer, S. B. Yi, D. Letzig, Effect of rare earth additions on microstructure and texture development of magnesium alloy sheets, Scripta Mater., 63 (**2010**) 7, 725–730, doi:10.1016/j.scriptamat.2009.12.033

[17] J. O. Park, C. H. Paik, Y. H. Huang, R. C. Alkire, Influence of Fe-rich intermetallic inclusions on pit initiation on aluminum alloys in aerated NaCl, J. Electrochem. Soc., 146 (**1999**) 2, 17–523, doi:10.1149/1.1391637

[18] Z. Wu, W. Zheng, G. Li, H. Matsuura, F. Tsukihashi, Effect of inclusions' behavior on the microstructure in Al-Ti deoxidized and magnesium-treated steel with different aluminum contents, Metall. Mater. Trans. B, 46 (**2015**) 3, 1226–1241, doi:10.1007/ s11663-015-0311-4

[19] T. R. Sippel, S. F. Son, L. J. Groven, Altering reactivity of aluminum with selective inclusion of polytetrafluoroethylene through mechanical activation, Propellants Explos. Pyrotech., 38 (**2013**) 2, 286–295, doi:10.1002/prep.201200102

[20] K. S. Vinoth, R. Subramanian, S. Dharmalingam, B. Anandavel, Mechanical and tribological characteristics of stir-cast Al-Si10mg and self-lubricating Al-Si10Mg/MoS2 composites, Materials and Technology, 46 (**2012**) 5, 497–501

[21] J. Zygmuntowicz, A. Miazga, K. Konopka, W. Kaszuwara, Metal particles size influence on graded structure in composite Al2O3-Ni, Materials and Technology, 50 (**2016**) 4, 537–541

[22] K. Ma, H. Wen, T. Hu, T. D. Topping, D. Isheim, D. N. Seidman, E. J. Lavernia, J. M. Schoenung, Mechanical behavior and strengthening mechanisms in ultrafine grain precipitation-strengthened aluminum alloy, Acta Mater., 62 (**2014**), 141–155, doi:10.1016/j.actamat.2013.09.042

[23] C. L. Williams, T. Sano, T. R. Walter, J. Bradley, L. J. Kecskes, The role of second phase intermetallic particles on the spall failure of 5083 aluminum, Journal of Dynamic Behavior of Materials, 2 (**2016**) 4, 476–483, doi:10.1007/s40870-016-0082-2